Article:
Ettelaie, R, Khandelwal, N and Wilkinson, R (2014) Interactions between casein layers adsorbed on hydrophobic surfaces from self consistent field theory: kappa-casein versus para-kappa-casein. Food Hydrocolloids, 34. 236 - 246. ISSN 0268-005X

https://doi.org/10.1016/j.foodhyd.2012.09.006

Interactions between casein layers adsorbed on hydrophobic surfaces from self consistent field theory: κ-casein *versus* para-κ-casein

Rammile Ettelaie*, Niharika Khandelwal and Rosemary Wilkinson

School of Food Science and Nutrition, University of Leeds, Leeds, LS2 9JT, UK

*Corresponding author. Tel: +44 113 343 2981, E-mail address: r.ettelaie@leeds.ac.uk

Abstract

Interactions mediated by layers of κ-casein and para-κ-casein have been calculated and compared using the self consistent field (SCF) approach, at pH and electrolyte concentrations found in milk. Our results show the interaction potentials at close separation distances to be repulsive for κ-casein, while they are attractive for para-κ-casein. We have also studied κ-casein chains stripped of their sugar moieties and highlighted the important role that the carbohydrate side chains play in the provision of steric forces. The point of transition from a repulsive to an attractive interaction is found to be rather sensitive to the degree of coverage of the surface by the protein chains. At Γ=0.0025 chains per unit monomer area, the value is just over 40%, whereas at Γ=0.0032 this increases to 87%. At the coverage values higher than those we estimate for the surface of casein micelles, no transition is detected and the interactions remain repulsive even when all of κ-casein has been converted to para-κ-casein, as already shown by Mellema, Leermakers, & de Kruif (1999). At lower surface coverage values, the interaction potential curves for otherwise uncharged surfaces, covered with para-κ-casein, posses an energy barrier. We have demonstrated that the origin of this energy barrier is electrostatic, with para-κ-casein contributing a net positive charge to the surface. We have also explored the importance of the asymmetry in the distribution of charge between the para-κ-casein and the glycomacropeptide sides of the protein. The glycomacropeptide is net negative while para-κ-casein side is net positive at neutral pH. Our results suggest that on a negatively charged surface, such as the surface of casein micelles, this uneven distribution of charge is just as important in determining the conformation of κ-casein chains as is the difference in the hydrophobic and hydrophilic nature of the two sides of this protein.

Keywords: Casein micelles, Renneting, SCF calculations, κ-casein and para-κ-casein, hydrocarbon side chains

1. Introduction

A knowledge of the structure of casein micelle aggregates in milk, and factors that contribute to their stability, are the corner stone of much of our scientific understanding of the processes that underline the manufacturing of some of the most important food products (Cooper, Corredig, & Alexander, 2010; Dalgleish & Corredig, 2012). These include such commonly encountered everyday foods as cheese (Fox, McSweeney, Cogan, & Guinee, 2004), yogurt, yogurt based drinks and desserts, and of course treated milk itself. In the last few decades, our insight into the structure of casein micelles has continued to improve as an increasing array of techniques such as atomic force microscopy (Ouanezar, Guyomarc'h, & Bouchoux, 2012), diffusing wave spectroscopy (Alexander, Rojas-Ochoa, Leser, & Schurtenberger, 2002), transmission electron and field-emission scanning electron microscopy (Dalgleish, Spagnuolo, & Goff, 2004; Kalab, 1993; Lucey, et al., 1996), dynamic light scattering (Dalgleish & Hallett, 1995) , small angle X-ray and neutron spectroscopy (de Kruif, Huppertz, Urban, & Petukhov, 2012), NMR (Bak, Rasmussen, Petersen, & Nielsen, 2001) and acoustic and electroacoustic spectroscopy (Gulseren, Alexander, & Corredig, 2010), have all been applied to probe the behaviour of casein micelles ever more deeply. Not surprisingly, as more data has become available, our view of the structure of casein micelle has also evolved. Over the same period, several different competing models, attempting to reconcile and explain a growing body of diverse experimental observations have emerged (Dalgleish, 2011). Despite some fundamental differences between these different models (Farrell, Malin, Brown, & Qi, 2006; Horne, 2006), and various revisions that have been made to them over years, a strikingly common feature that has remained the same is the role that κ-casein (KC) plays in providing colloidal stability to casein aggregates. It is envisaged that most, if not all of KC fraction resides at the surface of casein micelles. The protein κ-casein lacks the necessary number of phosphoseryl groups that otherwise allow α and β casein to participate in formation of calcium phosphate bridges between these molecules. Originally proposed by Walstra (1979), it is accepted that the function of KC is to provide sufficient steric repulsion between casein micelles to keep them well dispersed. In doing so, it prevents the aggregation of micelles and their subsequent phase separation from the milk serum. In this way milk delivers the required amount of calcium phosphate to infant through casein micelles, far in excess of what would otherwise be possible on the basis of solubility of calcium phosphate alone.

Common with other casein fractions, κ-casein is a proline rich, natively disordered protein with a small amount of secondary structure and no tertiary structure (Dalgleish, 2011). In the models used in this work we shall make extensive use of this fact, essentially arguing that the presence of this small amount of secondary structure is not an essential feature necessary for the functionality of KC, at least in so far as colloidal aspects of casein micelles are concerned. Bovine κ-casein comprise of 169 amino acid residues of which around 44% can be considered as being hydrophobic (Mercier, Brignon, & Ribadeau.B, 1973). It is also a glycoprotein, with around three or four short glycosidic chains, each consisting typically of 3 or 4 sugar moieties attached to threonyl residues in positions 131,133,135 and 142, and serine one in position 141, counted along the protein backbone from its N-terminus(Swaisgood, 2003). During renneting processes, the enzyme chymosin hydrolyses the bonds between phenylalanine and methionine residues (105-106) to split the κ-casein into two separate chains. The chains are thought to have distinctly different degrees of hydrophobicity. The C-terminus portion consisting of residues 105-169, the glycomacropeptide (GMP), is hydrophilic and upon renneting leaves the surface of the micelles to dissolve into milk serum. The rest of the κ-casein, para-κ-casein (PKC) made up of residues 1-105, remains on the surface of the micelles but is considered too hydrophobic to be able to provide the necessary steric forces to keep the casein micelles apart. This leads to the aggregation of the micelles and curdling of the milk; probably the most crucial step in the manufacturing of cheese. Thus, for the intact KC, it is the glycomacropeptide portion which protrudes away from the surface of micelles and leads to the repulsive interactions between the micelles as they approach each other too closely (Walstra, 1979). It is perhaps surprising then to note that a simple count of the number of hydrophobic residues, without considering the relative degree of hydrophobicity of each, indicates a very similar proportion of such amino acids on both the glycomacropeptide (47%) and para-κ-casein (47%) sides of KC. Therefore, GMP must owe a large degree of its hydrophilicity to the presence of sugar moieties, all of which reside on this section of κ-casein. Of course, glycosylation of a protein is not a sufficient condition for it to become a superior steric stabiliser, as was demonstrated recently by our SCF calculations involving protein + polysaccharide conjugates (Akinshina, Ettelaie, Dickinson, & Smyth, 2008). Such conjugates are produced through the Maillard reaction between these two sets of biopolymers, with the view of producing better food grade emulsion stabilisers (Akhtar & Dickinson, 2007; Dickinson & Semenova, 1992). Our calculations were performed for α_{s1}-

casein reacting with polysaccharide chains of various lengths, attached to it at various different points along its backbone. We found that for a long polysaccharide chain, irrespective of where it was attached to α_{s1}-casein, the conjugate layers always provided a stronger steric interaction between two surfaces, when compared to the pure protein layers. However, when the polysaccharide side chain was made much smaller than α_{s1}-casein, the results became dependent on the location of the attachment. The steric forces mediated by the conjugate were once again more repulsive if the glycosylation occurred towards either end of the protein, where α_{s1}-casein has its more hydrophobic sections. But more interestingly, when the attachment was made to the more hydrophilic middle part of the protein, the conjugate proved less efficient as a steric stabiliser than unmodified α_{s1}-casein (Akinshina, et al., 2008).

Most calculations in the past, attempting to study the nature of forces mediated by KC surface layers on the surface of casein micelles, assume from the onset that the glycomacropeptide part of the KC can be modelled as a hydrophilic, homopolymer polyelectrolyte (de Kruif & Zhulina, 1996; Tuinier & de Kruif, 2002). However, in the light of the discussion presented above, it seems useful to examine this assumption in more detail by including some of the features of the primary sequence structure of the κ-casein in the calculations. In one of the very few studies of this type, Mellema, Leermakers and de Kruif (1999) applied the self consistent field (SCF) approach to models of κ-casein and para-κ-casein in which, the amino acid residues comprising the chains, where divided into a number of distinct groups based on their degree of hydrophobicity and their electrical charge (pK_a values). As expected, the interactions provided by KC layers were found to be strongly repulsive. What was more surprising was that PKC layers also mediated repulsive forces between the micelles, although they were somewhat shorter ranged than those obtained for KC. The authors concluded that the repulsion by PKC layers was sufficient to overcome any attractive van der Waals interactions between the micelles (Mellema, et al., 1999). We believe that this result arises due to an overestimation of the degree of surface coverage of casein micelles by KC. At the coverage level used in this work, the configuration of KC chains is highly deformed from one adopted by a single chain adsorbed/grafted on the surface (i.e. low coverage limit). The lateral excluded volume interactions between chains, causes KC to stretch away from the surface forming so called "brush" layers. In general, the overlap between two such interfacial "brush" layers produces very strong repulsion. Even when KC

chains are replaced by shorter PKC ones the coverage is still high enough to lead to the formation of "brush like" configurations, and thus repulsive forces. It turns out that the nature of interactions produced by κ-casein layers, even on a qualitative level, is rather sensitive to the choice of surface coverage one uses. We shall discuss this point in more detail later.

Self consistent field calculations have been successfully applied to compare the configurations adopted by α_{s1}-casein and β-casein at interfaces (Dickinson, Horne, Pinfield, & Leermakers, 1997; Leermakers, Atkinson, Dickinson, & Horne, 1996). The calculations predict surface density profiles for proteins in good agreement with data obtained using neutron reflectometry (Atkinson, Dickinson, Horne, Leermakers, & Richardson, 1996). Similarly, the results provided a clear explanation of the observed superior stability of β-casein stabilised emulsions compared to α_{s1}-casein (Dickinson, Pinfield, Horne, & Leermakers, 1997). Parkinson, Ettelaie and Dickinson (2005) used SCF approach to explain the observed enhancement in the steric stabilizing capacity of casein at very low surface converge, when this is combined with a thin dense layer of another protein, such as β-lactoglobulin also present at the interface. Self consistent field calculations have also been used to investigate the structure of mixed protein + polysaccharide films (Ettelaie, Akinshina, & Dickinson, 2008, 2009). The work highlighted the importance of the non-uniform distribution of polysaccharide charge in the formation of true "equilibrium" multi-layers. The study also provided an explanation of the reversal of the interfacial charge during the deposition of polysaccharide, in absence of any specific short ranged interactions between protein and polysaccharide, hitherto thought to be essential in formation of such multi-layers (Patel, Jeon, Mather, & Dobrynin, 2006). Self consistent field calculations have also been applied to non-food related proteins such as neurofilament proteins (Zhulina & Leermakers, 2007, 2009).

In the following section we shall outline our SCF methodology before we describe our models for the KC and PKC. Next, we consider the interactions that are produced due to the overlap of layers of these proteins between two smooth, hydrophobic surfaces. The surfaces are also assumed to be uncharged by themselves. We stress that this is a gross simplification for the structure of the surface of casein micelles. It ignores the presence of other components, such as α and β-casein, calcium phosphate particles, and not least water. Thus, the hydrophobicity of the surface of micelles is quite likely to be rather heterogeneous. There

is also some evidence to suggest that the surface of casein micelle is far from being smooth (Dalgleish, 2011; Donnelly, McNeill, Buchheim, & McGann, 1984). Even more significant is the presence of other casein fractions on the surface, which implies additional surface charges beside those arising from KC (or PKC for renneted micelles). In a more detailed model of surface of casein micelles, these extra charges have to be correctly accounted for. However, while it is relatively easy to calculate the overall surface charge of the micelles, for example using the reported ζ-potential values in the literature (Dalgleish, 1984), it is not so trivial to determine how much of this charge should be attributed to κ-casein and what percentage is the result of other casein fractions on the surface. In the present study then we shall purely focus on the interactions that are directly due to KC or PKC and defer the treatment of some the points raised to future work. We believe that this is still a useful exercise, since in the absence of some of these additional complications, it is more revealing to compare the behaviour of κ-casein covered interfaces with those covered by para-κ-casein. In this sense the surfaces used in the present study are more representative of those for the emulsion droplets. Finally before the conclusion section, we also attempt to relate the nature of the interactions mediated by KC and PKC to different configurations that each of these proteins adopt at interfaces.

2. Methodology

Our SCF calculations are based on the approach originally proposed by Scheutjens and Fleer (1980, 1982) for homopolymers and later extended to co-polymers consisting of different type of monomers (Evers, Scheutjens, & Fleer, 1990) . In this approach, the space between two approaching surfaces planar surfaces is divided into a set of layers parallel to the surface. Each layer has a thickness a_0, where a_0 = 0.3 nm is the nominal size of the monomers, the ions and the solvent molecules. The layers themselves are further sub-divided into equal sized cells, defining an underlying lattice upon which the calculations are performed. For a cubic lattice the volume of each cell is $(a_0)^3$. Cells are either occupied by monomer residues, belonging to KC (or PKC), by free ions or by solvent molecules. No lattice site can remain empty, thus imposing the incompressibility condition for the solution as a whole. This also implies that the total number density of all species per unit cell has to add up to exactly 1 everywhere, and that the volume fraction of each species in a layer is the

same as its number density in that layer. Therefore, we shall use the term number concentration and the volume fraction interchangeably through this paper.

The central quantities in SCF calculations are a set of Green's functions, known as segment distribution functions, $G^c(s,z)$ and $G^n(s,z)$. The quantity G(s,z) represents the probability, to within a constant pre-factor, that a chain consisting of only the first s segments of KP will end in layer z. The first s monomer residues are taken from the C-terminus end of the protein for $G^c(s,z)$ and from the N-terminus end for $G^n(s,z)$. The layer number z runs from 1 to L, where La_0 is the separation distance between the two planar surfaces. The connectivity of the chains implies that two consecutive monomers s-1 and s have to either reside in two neighbouring layers or else be in the same layer. This leads to the following recurrence relation for $G^{\omega}(s,z)$:

$$G^{\omega}(s,z) = \exp(-\psi_{t_{\omega}(s)}(z))\left(\lambda_{-1}G^{\omega}(s-1,z-1) + \lambda_0 G^{\omega}(s-1,z) + \lambda_{+1}G^{\omega}(s-1,z+1)\right) \quad , \qquad (1)$$

where ω is set to n or c depending on which end of the KC (or PKC) the first s residues are counted from. The parameters λ_{-1}, λ_{+1} and λ_0 are related to the number of possible nearest neighbours that a residue can have in the layers before, after and in the same layer as itself. For the cubic lattice used here, $\lambda_{-1} = \lambda_{+1} = 1/6$ and $\lambda_0 = 4/6$. A protein chain, such as PKC or KC, will consist of different types of residues. We define operators $t_c(s)$ and $t_n(s)$ such that they specify the type of monomer to which the s residue, counted from the appropriate end along the protein backbone, belongs. Obviously, $t_c(s) = t_n(N-s+1)$ for any protein, where N is the total number of monomer residues comprising the chain. In principle, $t_c(s)$ and $t_n(s)$ can specify any of 20 or so different amino acid types that make up the protein chains. However, following Leermakers et al. (1996), we classify similar amino acids into a smaller number of groups where possible, as detailed in the next section.

Another important quantity in Eq. (1) is the mean potential $\psi_i(z)$ acting on species i in layer z. The potential $\psi_i(z)$ represents the sum of interactions that a monomer of type i, located in position z, will have with other monomers, solvent molecules and ions:

$$\psi_i(z) = \left(\chi_{i\sigma}(\delta_{z,1} + \delta_{z,L})\right) + q_i\psi_{el}(z) + \psi_h(z) + \left[\sum_j \chi_{ij}\left(<\phi_j> - \phi_j^b\right)\right] \quad . \qquad (2)$$

The last term in Eq. (2) arises from the presence of short ranged, nearest neighbour, interactions. The strength of such an interaction between two species of types i and j is specified through the usual Flory-Huggins χ parameter, χ_{ij}. Large positive values of χ_{ij} are enthalpically unfavourable, while negative values indicate a favourable interaction between i and j. The summation j in Eq. (2), runs over all monomer kinds, ions and solvent. The possibility of any given monomer of type i situated in layer z, having contacts with monomers of type j, is related to the local density of the latter:

$$< \phi_j (z) > = \lambda_{-1}\phi_j (z-1) + \lambda_0 \phi_j (z) + \lambda_{+1}\phi_j (z+1) \quad . \qquad (3)$$

The quantities $\phi_j(z)$ and ϕ_j^b in Eq. (2) denote the volume fraction of species j in layer z and in the bulk solution, respectively. The value of $\phi_j(z) = 0$ for $z < 1$ and $z > L+1$ for all species j. The weighted average $<\phi_j(z)>$, defined by Eq. (3), takes into account the number of possible neighbours in each layer around z. Since we shall assume that all κ-casein and para-κ-casein chains always remain on the surface of the micelles (i.e. are essentially grafted), the bulk concentration of monomers belonging to these protein chains will be zero. For ions, their bulk concentration specifies the background electrolyte concentration in the solution. The protein chains, as well as ions and solvent molecules, are subjected to Brownian motion. As a result, local densities, $\phi_j(z)$, will fluctuate about their mean values. The mean field nature of our calculations arises from the neglect of such fluctuations. However, for relatively dense interfacial layers, this is known to be a good approximation (Fleer, Cohen Stuart, Scheutjens, Cosgrove, & Vincent, 1993; Grossberg & Khokhlov, 1994). Furthermore, since all cells at the same distance away from the surfaces (i.e. within the same layer) are identical, the neglect of fluctuations implies that they will have exactly the same values of fields, $\psi_j(z)$, and densities, $\phi_j(z)$. Monomers and other species also interact with the planar surfaces. Again the strengths of these interactions are specified using Flory-Huggins parameters $\chi_{i\sigma}$, where negative values indicate the tendency for a monomer species i to adsorb onto the interface. These interactions only arise for monomers which reside in the two layers adjacent to the walls, z=1 and z=L. This is indicated in Eq. (2) through the use of Kronecker delta functions $\delta_{z,1}$ and $\delta_{z,L}$, where $\delta_{lk} = 1$ if l=k, and zero otherwise.

Eq. (2) accounts for other interactions apart from the short-range nearest neighbour ones. The electrostatic interactions between all charged species is represented by the term $q_i \psi_{el}(z)$

in Eq. (2), where q_i is the electrical charge of species i and $\psi_{el}(z)$ the electrostatic potential at layer z. The electrostatic potential is determined itself by the distribution of charged species through Poisson equation

$$\nabla^2\psi_{el} = \frac{-\rho}{\varepsilon_r\varepsilon_0} = -4\pi\gamma\sum_j q_j\phi_j(z) \quad . \qquad (4)$$

We express all charges in unit of electronic charge e, and the electric potentials in units of k_BT/e, where T is the temperature and k_B the Boltzmann constant. With unit of length also set to a_0, the constant γ in the above equation becomes the ratio of Bjerrum length, $e^2/(4\pi\varepsilon_r\varepsilon_0 k_BT)$, to the monomer size, a_0. The remaining contribution to the mean fields in Eq. (2) is a hard core potential term, $\psi_h(z)$, having the same value for all species. This contribution arises from the requirement that all cells should be occupied, namely $\sum_j \phi_j(z) = 1$ for every layer z, as was mentioned previously.

Once the mean field potentials are available, Eq. (1) can be used to calculate the segment distribution functions. The values for G(1,z) needed to start the recurrence depend on whether a chain is free or grafted, and for the latter case the end from which the segment distribution function is specified from. For κ-casein, it is the N-terminal end, i.e. the para-κ-casein side, which needs to be taken as being grafted to the surface. For this, the first segment has to be in contact with one of the walls. Therefore

$$G^n(1,z) = (\delta_{z,1} + \delta_{z,L})\exp(-\psi_{t_n(1)}(z)) \quad , \qquad (5a)$$

with Kronecker delta functions ensuring that for all layers not adjacent to the walls $G^n(1,z)=0$. For the free, C-terminus end, we simply have

$$G^c(1,z) = \exp(-\psi_{t_c(1)}(z)) \quad . \qquad (5b)$$

The knowledge of segment distribution functions allows one to calculate various thermodynamic quantities of interest such as the free energy of the system as a function of the separation distance, d, between the plates. In particular, they also allow one to determine the volume fraction of each species in different layers, at various distances away from the

surface. This is obtained through the so called the compositional law (Evers, et al., 1990; Fleer, et al., 1993)

$$\phi_j(z) = \frac{2\Gamma \sum_{s=1}^{N} G^n(s,z)\, G^c(N-s+1,z)\, \delta_{j,t_n(s)}}{\exp(-\psi_j(z)) \sum_{z=1}^{L} G^n(N,z)} \quad . \qquad (6)$$

The quantity $(\sum_{z=1}^{L} G^n(N,z) = G^c(N,1) + G^c(N,L)$ appearing in Eq. (6), is twice the single chain partition function for a KC (or PKC) molecules grafted to a surface, with N being the total number of the amino acid residues making up the chain. The coverage of the surface by KC or PKC, in units of grafted chains per monomer unit area a_0^2, is denoted by Γ. We assume that the two approaching surfaces are identical and have the same level of chain coverage.

It is evident from Eqs. (1) and (6), that in order to calculate the segment distribution functions and the values of $\phi_j(z)$, one needs the mean fields, $\psi_j(z)$. However, as seen from Eqs. (2) and (4), the values of these fields are in turn determined by the spatial distribution of different species, $\phi_j(z)$, at the interfacial region. To overcome this problem then, we implement an iterative procedure in which one begins with a set of guess initial values for $\psi_j(z)$. Next, the segment densities that result from these initial fields are calculated. The segment volume fractions obtained are substituted in equations (4) and (2) to yield improved values for the mean fields. This procedure is repeated in the same manner until a "self consistent solution", to a desired level of accuracy, is obtained. It can be shown that the solution thus obtained corresponds to a set of density profiles that minimise the free energy of the system (Grossberg, et al., 1994). The value of this minimum free energy is given by the following equation (Ettelaie, Murray, & James, 2003; Evers, et al., 1990; Fleer, et al., 1993):

$$\Delta F = -2\Gamma \ln\left(\frac{1}{2}\sum_{z=1}^{L} G^{n}(N,z)\right) - \sum_{k}\sum_{z=1}^{L}\left(\phi_k(z) - \phi_k^b\right) - \sum_{j}\sum_{z=1}^{L}\psi_j(z)\phi_j(z)$$
$$+ \frac{1}{2}\sum_{i,j}\sum_{z=0}^{L+1}\chi_{ij}\left(\phi_j(z) - \phi_j^b\right)\left(<\phi_i(z)> - \phi_i^b\right) - \sum_{i,j}\chi_{ij}\phi_i^b\phi_j^b$$
$$+ \frac{1}{2}\sum_{j}\sum_{z=1}^{L}\psi_{el}(z)q_j\phi_j(z) + \sum_{j}\chi_{j\sigma}(\phi_j(1) + \phi_j(L))$$

. (7)

As before, summations over indices i and j include all species, whereas the one over index k is limited to the free species only, i.e. just ions and solvent molecules in the present system. Extension of the method to branched polymers or polymers with side chains is relatively straightforward and has been described elsewhere (Ettelaie, et al., 2003; Fleer, et al., 1993).

3. Models for κ-casein and para-κ-casein

An implicit assumption in the use of SCF theory is the premise that a polymer chain is free to adopt any of the many conformations available to it in accord with the appropriate Boltzmann probability distribution. For globular proteins, this "ergodicity assumption" is known not to apply. Globular proteins, trapped in their native state, only sample a very small fraction of different possible configurations. In contrast, for "rheomorphic" proteins such as casein (Dalgleish, 2011) or denatured globular proteins, the use of SCF method is more feasible.

In order to reflect the nature of the primary sequence of κ-casein in our calculations we follow the approach of Leermakers et al. (1996) in dividing the amino acid residues into a few distinct groups. Although it is entirely feasible to represent each type of amino acid individually, this leads to a proliferation of parameters entering the model without providing much additional insight into the interfacial behaviour of κ-casein. Here, we use five groups representing hydrophobic, polar but uncharged, negative and positively charged amino acids. The fifth group consists of histidine, which due to its somewhat different pK_a is placed in a group of its own, distinct from other charged residues. A schematic diagram showing the primary sequence of κ-casein (Jolles & Fiat, 1979), classified according to our five groups is illustrated in Fig. 1. The hydrophobic, polar or charged nature of amino acids belonging to

each group is specified in the model through the interactions that these have with ions, solvent and of course other groups. Thus for example, hydrophobic group (group 1) has an unfavourable set of χ interaction parameters, ranging from 1.0 and 2.5 (in units of k_BT), with solvent and various other charged and hydrophilic groups. On the other hand, the same group has a short range interaction with the surface indicating an adsorption energy of 2 k_BT per monomer ($\chi = -2$). These values are typical of hydrophobic interactions (Hunter, 1989) and as with other parameters in the model are essentially those used in similar previous studies (Ettelaie, et al., 2008; Leermakers, et al., 1996). A full list of all the χ parameters, as well as the pK_a values for the charged groups is provided in Table 1.

The charge of ionisable groups is calculated as usual based on their pK_a value and the pH of the bulk solution. When the bulk pH is close to the pK_a value for a group, the charge of the species in that group can alter due to the variation of local pH close to the interface. For neutral pH, this is only significant for members of group 4, i.e. histidine. Since κ-casein only contains three such residues, we shall ignore this effect in our calculations. Table 1 also indicates the presence of a carbohydrate group (group 6) in the model. The glycoprotein κ-casein is known to contain three or four carbohydrate moieties, attached to its threonyl and the single serine residues between positions 131 to 142 (Swaisgood, 2003). The moieties are each made up of three or four sugar groups (see Fig. 1). For simplicity, we shall represent all such side chains as being linear. Furthermore, due to close proximity of the attachment of the glycosidic side chains along the κ-casein backbone, we shall model all the carbohydrate chains as being linked to the same residue of κ-casein, namely residue 142. The sugar groups, comprising the glycosidic side chains, make up the monomers in group 6 of Table 1. The strong hydrophilic nature of these monomers is reflected by their strong affinity for solvent, as indicated by a χ interaction parameter of -1 (k_BT) between these and water molecules.

Other important parameters in our model are the electrolyte concentration and the degree of surface coverage by κ-casein chains. The volume fraction of the electrolyte was chosen as 0.0015, which is roughly equivalent to a concentration of 0.05 mol/l. This is within the range of values reported for milk. We assume that ions making up the electrolyte are symmetrical monovalent ions. Casein micelles have a rather broad size distribution with an average size of 200 nm. It has been estimated that the number of protein chains in a micelle is of the order of 10000 (Dewan, Chudgar, Mead, Bloomfield, & Morr, 1974). Assuming that 10 to 15% of

these chains are κ-casein, and that all these molecules are on the surface of the micelle, then for a micelle of typical size the value of the surface coverage is Γ=0.0007 chains per monomer unit area. If instead the smallest micelles in the size range, reported to be around 80nm (Dewan, et al., 1974), are considered then a value of 0.0045 chains per (a_o^2) for Γ is obtained. It is seen that even in the latter case, the estimated coverage of surface by KC chains is substantially lower than the value of Γ=0.024 chains per (a_o^2), used in the previous SCF study of KP and PKC covered surfaces (Mellema, et al., 1999). We consider a value of Γ=0.0025 chains per monomer unit area in this study. For high degrees of coverage, the chains in the interfacial layer, even for para– κ-casein case, are in highly stretched "brush" like conformations (Fleer, et al., 1993). The overlap of such "brush" like layers always induces strong steric repulsion between two surfaces. This was indeed seen to be the case for the calculations of Mellema et al. (1999). Their result showed, that at high values of Γ, the steric repulsion produced by both KC and PKC layers was more than enough to overcome the van der Waals attraction. They also concluded that the results were not particularly sensitive to the amount of background electrolyte. This is again expected, since the stretching of chains is due to excluded volume repulsion between densely grafted chains, rather than any electrostatic repulsion between them.

Following the process of renneting, we only retain the first 105 monomers in our model κ-casein like chain. The position of broken peptide bond is indicated in Fig. 1. Partial renneting is simulated by having a mixture of both PKC and KC grafted on the surface. We also investigate the importance of glycosidic side chains in provision of steric repulsion by κ-casein, by considering hypothetical KC chains without their carbohydrate groups.

4. Results and discussion

The interaction potential between two surfaces, arising from the overlap of their protein interfacial layers, is calculated by considering the changes in the free energy of the system $F(r) - F(\infty)$. The free energies at a separation distance of r and when the plates are infinitely apart, F(r) and $F(\infty)$, are obtained using Eq. (7). In practice we set $F(\infty) = F(100)$. At a separation distance of r=100 monomer units the two interfaces are sufficiently isolated so as not to affect the adsorption behaviour of each other. Increasing r beyond this distance produces no appreciable changes in the value of the free energy of the system.

The graphs in Fig. 2 display the SCF calculated interaction potentials per unit area (in units of k_BT/ a_o^2) plotted against the distance between the two surfaces (measured in units of a_o). The graphs are for adsorbed layers of KC, PKC, and KC without its carbohydrate side chains. We shall refer to the latter as modified κ-casein (MKC). Each curve only includes the potential mediated by the corresponding protein, without the addition of other existing colloidal forces. The van der Waals interaction between the two parallel plates is displayed separately by the short dashed line in Fig. 2, for comparison. This interaction is given by $V_{vw}(r) = - A / (12\pi r^2)$ for two parallel plates (Hunter, 1989). An accurate value for the Hamaker constant, A, of casein micelles, dispersed in water, has not been determined as far as we are aware, but it is expected to be of the order of a k_BT. We have taken this to be 1 k_BT, similar to that for oil emulsion droplets. All the results were obtained at neutral pH and with a background electrolyte volume fraction of 0.0015. This sets the Debye length in the solution to ~ $4.5a_o$. Also as mentioned in the previous section, the protein surface coverage is Γ=0.0025 chains/ a_o^2 for all the three cases studied. The first obvious feature of the graphs in Fig. 2 is that at very close separation distances, the interaction potentials arising from κ-casein is seen to be positive. That is to say that close to the point of contact between the surfaces the interaction is repulsive. In contrast, for para-κ-casein and modified κ-casein without its sugar moieties, the interactions at the same short distances are attractive. We presume that this is a reflection of the more hydrophobic nature of para-κ-casein and that of κ-casein stripped of its carbohydrate side chains, where interfacial protein layers prefer to be in contact with each other rather than with the water molecules. They may also be indicative of some degree of bridging at these levels of protein surface coverage. Thus, this result seems to suggest that the glycopeptides nature of κ-casein is an important factor in providing the functional properties of this protein. At larger distances, the interaction potential remains repulsive for KC and continues to be strong enough to overcome the van der Waals attraction (Fig. 2). We shall see that this is also the case at somewhat higher salt concentrations. The effects of the addition of salt on the colloidal behaviour of the system will be discussed further below.

So far the above findings are in line with the classical view of κ-casein as a colloidal stabiliser of casein micelles. Where our data begins to show some unexpected results is in the interaction curve obtained for the para-κ-casein at slightly larger surface separations of r = 4.5 to $13a_o$. At these distances, we find that the interaction potential mediated by para-κ-

casein exhibits a repulsive energy barrier. For our model PKC, the height of this energy barrier is 0.0023 k_BT/ a_o^2 per unit area, occurring at $r \sim 6a_o$. In fact, careful inspection shows that the potential curve for MKC layers also has this energy barrier, although this is considerably smaller and occurs at a slightly larger distance of $r \sim 8a_o$. Two points are worth stressing at this stage. Firstly, the two surfaces used in our calculations have no charge of their own. The surface charge is therefore solely due to the presence of para-κ-casein. The importance of this point will become clear shortly. The second point is that the interaction potential for PKC has a close resemblance to the combined attractive van der Waals and repulsive electrostatic potential curves seen in the classical DLVO theory of colloidal stability (Hunter, 1989). We have not included the van der Waals forces in the graph of the potential for PKC, but such an attraction is present due to bridging or hydrophobic nature of PKC as was mentioned above. This then leaves us with a repulsive component, which from the shape of the interaction potential graph for PKC in Fig. 2 looks more likely to be electrostatic, rather than steric. To test this idea we repeat the calculations of Fig. 2 at higher salt concentrations. The results of this exercise are presented in Fig. 3, where now the background electrolyte volume fraction is 0.0045, correspondingly roughly to a salt concentration of 0.15 mol/l. The graphs are plotted to the same scale as those in Fig. 2. We find that the interactions mediated by KC are not grossly affected by the addition of salt. Although between distances of $r=6a_o$ to $8a_o$ a small energy minimum is now detectable, the interactions due to overlap of KC layers remain strongly repulsive at shorter distances. The relative indifference of this repulsive force to the presence of salt is a good indication of its steric nature. The effect of electrolyte addition is much more dramatic on interactions between PKC covered surfaces. It is obvious that more salt has all but removed the energy barrier in the PKC mediated interactions. The interaction potential due to para-κ-casein layers is now purely attractive. Thus, unlike KC, it seems that the repulsion produced by PKC in graph of Fig. 2 has indeed electrostatic origins. Further evidence in support of this view can be obtained by considering the electric potential in the interfacial region. Graphs in Fig. 4 show the spatial variation of electric potential, $\psi_{el}(r)$, as calculated by Poisson equation Eq. (4), with the distance away from the surface for KC and PKC covered interfaces. For the former, our calculated surface potential is around $\psi_{el} \sim -13$ mV, slightly lower than the experimentally determined ζ-potentials values of −18 to −20 mV, reported for casein micelles in the literature (Dalgleish, 1984; Wade, Beattie, Rowlands, & Augustin, 1996). This is not

surprising since we have not included any additional negative charges contributed by α and β-casein, which of course also form part of the surface of the micelle. It is clear that the electric potential has a larger magnitude for surfaces covered by para-κ-casein than those for κ-casein. More interestingly, it is seen that the magnitude of surface potential is larger for PKC than that calculated for KC. Also the sign of the surface electric potential is positive for PKC as oppose to being negative for KC. Clearly surfaces covered by para-κ-casein seem to be more charged than those covered with κ-casein according to this result. In the absence of the steric repulsion by PKC, the interaction potential curve induced by the overlap of layers of this protein, show a distance dependence variation expected from a combination of an attractive force + electrostatic repulsion, as seen to be the case in Fig. 2. Before we more closely examine the reasons for the emergence of such positively charged PKC covered surfaces, it is worth speculating on the effect that any additional surface charge from α and β-casein may have on this result. Since this charge is negative, it will tend to reduce the surface potential of the interface covered by PKC, and may well even neutralise the positive charge of the surface completely. In other words, while the presence of α and β-casein will enhance the electrostatic component of the repulsion for κ-casein covered micelles, it will have the opposite effect for renneted ones, with para-κ-casein on their surface. This in turn should make the renneted micelles more prone to aggregation. Indeed, if the positive charge is not entirely neutralised, this might leave the interaction potential curve of Fig. 2 with a small energy barrier, not sufficient to prevent aggregation of the micelles, but large enough to account for the slow dynamics of such a process occurring during renneting.

A quick browse across the primary sequence of κ-casein in Fig. 1, reveals the distribution of charged amino acid groups between the glycomacropeptide part and the para-κ-casein side of the KC to be quite uneven. More specifically, the majority of positively charged residues, including all the histidine ones, reside on the para-κ-casein part of the protein. The presence of positive N-terminus on the para-κ-casein side and negatively charged C-terminus on glycomacropeptide only serves to further exaggerate this asymmetrical distribution of charge along the κ-casein backbone. To demonstrate the effects of this uneven distribution of positively charged groups, we have calculated the charge of the residues in each group, at several different pH values, using their corresponding pK_a as given Table 1. The total charge for KC and PKC chains are then calculated from the number of different types of residues

that comprise each of these proteins. The variations of charge with pH, for both KC and PKC portion of the chain, are plotted together in Fig. 5. At neutral pH, κ-casein is negatively charged with a pI = 5.6, in excellent agreement with experimental results. At the same pH = 7, para-κ-casein part of the protein is positively charged with a charge that is actually higher in magnitude than that of κ-casein itself. The charge of the para-κ-casein, at pH=7, is actually one electronic unit less than that in Fig. 5 (i.e. then the PKC portion of κ-casein). This is due to the formation of a new negatively charged C-terminus, following the breakage of the peptide bond by chymosin, between residues 105 and 106. The renneting then causes a large portion of negatively charged residues of κ-casein to be removed, as the detached glycomacropeptide leaves the surface of the micelles. But for the presence of additional negative charge, contributed by other casein fractions, the para-κ-casein covered surface would be positively charged. This is the case in our calculations, where in the absence of these other contributions, the positive charge on the surface leads to a sufficient amount of electrostatic repulsion, responsible for the presence of the energy barrier seen in Fig. 2.

Much insight can be gained on the conformations adopted by polymer chains by considering their volume fraction profile and the average distance of their monomers away from the interface. Self consistent field calculations, using very similar parameters to those used here, have confirmed the anticipated diblock type behaviour for β-casein (Dickinson, Horne, et al., 1997; Leermakers, et al., 1996). Similarly, a_{s1}-casein adsorbed at a hydrophobic interface has been shown to adopt a triblock configuration, with a middle loop section that protrudes away from the surface the two end parts that remain close to and lay relatively flat on the interface (Akinshina, et al., 2008; Dickinson, Horne, et al., 1997). It is interesting then to see what type of configuration is predicted by our calculations for κ–casein, grafted to the hydrophobic interface considered in this study. In Fig. 6 we have plotted the volume fraction of KC, PKC and κ-casein without its sugar moieties (MKC), as a function of the distance away from the surface. Not surprisingly the volume fraction of the shorter para-κ-casein is smaller than the other two proteins and it drops to zero at a distance of $3.5a_o$. The volume fraction of MKC is identical to that of KC for the first few layers next to the interface. The carbohydrate side chains on κ-casein only affect the volume fraction of the chains at distances further away from the interface. Although the volume fraction of both KC and MKC drop rapidly as one moves away from the surface, at a distance of $3a_o$ it is seen to be twice as high for KC as for MKC. At a distance of $4a_o$ the ratio is even larger, at just over three. We conclude that the

higher concentration of protein at a distance of a few layers away from the surface is clearly due to its sugar moieties. This again points to the important contribution that the carbohydrate part of the protein plays in providing the functional behaviour of κ-casein. That the outer part of the "hairy" κ-casein layer consists of these carbohydrate moieties is best demonstrated by the graph of Fig. 7a. In Figs. 7a and 7b, we have plotted the average distance away from the surface for each of the amino acid residues comprising the chains. The monomers are ranked 1 to 169, counting from the N-terminus side. While in Fig. 7a we show the result for KC, Fig. 7b displays this for MKC where the side chains have been deliberately removed. It is clear that the most extended part of the κ-casein is the section attached to the carbohydrate moieties. The inset in Fig. 7a shows a magnified version of the graph involving this section of the chain. In both the inset and the main graph itself we have also included the average distance from the surface for the sugar moieties comprising the side chains. This is represented by the dashed line. As mentioned before we model these side chains as four linear chains, each made of four sugar groups, all attached to the residue 142 of the κ-casein chain. For a real chain we expect the extension into the solution to be slightly less, but involving a slightly larger portion of the backbone, from residue 131 to 142, since the sugar moieties are distributed at different points along the chain in this section of the protein. Graph of Fig. 7b is even more revealing. It is clear that without these carbohydrate monomers, no clear part of the MKC can be identified as really extending into the solution. Even in the presence of these side chains, we find that the κ-casein has a conformation that can hardly be considered as being a diblock. Whereas similar calculations for β-casein have shown that one side of this protein extends well away from the wall, thus forming a tail (Dickinson, Horne, et al., 1997; Leermakers, et al., 1996), this is clearly not observed for κ-casein. Perhaps, considering the fact that the percentage fraction of hydrophobic residues on both PKC and glycomacropeptide sides of KC are roughly the same, this is not all that surprising.

Evidently κ-casein is not as good an emulsifier or steric stabiliser of oil emulsion droplets, at least in comparison with the other two casein fractions. Yet on the surface of micelles, it forms a hairy surface layer which is extremely effective in establishing the desired colloidal stability of the casein micelles. From the above results, we have seen that on hydrophobic surfaces with no charge of their own, κ-casein has a conformation that does not match the anticipated one where one end of chain forms a tail sticking away from the surface. The

thickness of the "hairy" layer we predict here is also much smaller than the reported data, putting this as much as 5nm. Can such a configuration then arise on the surface of the micelles? We believe the answer to be yes, given the uneven distribution of the charge of κ-casein. Recently, in an unrelated study, we have considered the effects of the heterogeneous distribution of the charge of polysaccharides on their adsorption behaviour in mixed interfacial layers of protein + polysaccharide (Ettelaie, Akinshina, & Maurer, 2012). It was found that polysaccharides with short negative highly charged sections and longer lightly charged parts formed a significantly more extended interfacial layer, compared to chains with a uniformly distributed charge along their backbone, when adsorbed on top of a positive protein layer. The heterogeneously charged polysaccharides had their lightly charged tails protruding far into the solution, away from the wall. There is some analogy with this situation here. As we have seen from Fig. 5, the distribution of the charge is not symmetrical for κ-casein, with a more negative charge located on glycomacropeptide, leaving the para-κ-casein side of the molecule more positive at neutral pH. If the surface of the micelle already possesses some negative charge arising from other casein fractions, it will tend to repel the glycomacropeptide part of KP, while at the same time it will attract the positively charged para-κ–casein end. This then should lead to the same type of extended interfacial layers we had observed for the non-uniformly charged polysaccharides (Ettelaie, et al., 2012). Currently SCF calculations, involving κ-casein grafted to surfaces carrying a negative charge, are underway to test this idea.

Graphs in Fig. 2 show the interaction potentials mediated by KC and PKC, i.e. at the start and at the end of renneting process. In Fig. 8 we display the results for the intermediate stages, where only a fraction of KC is replaced with PKC. The label for each graph indicates the percentage of renneted chains. The total number of both proteins is maintained at Γ=0.0025 chains per monomer area, with pH=7 and the electrolyte volume fraction set to 0.0015 (about 0.05 mol/l), as before. With 20% of chains converted to PKC, it is seen that the potential curve develops a small minimum. Nevertheless, at very short plate separations the interaction is still strongly repulsive. As the renneting progresses further to 40%, the depth of the minimum in the potential energy becomes more pronounced. At 60% renneting the interactions are now attractive close to the point of contact between the two plates. We suspect that at this point the net negative charge of remaining KP chains and the positive charge contributed by renneted PKC molecules produce an almost neutral surface. With even

more renneting (see Fig. 8, the 80% graph), the surface begins to become positively charged. Although at short separations the forces are strongly attractive, the presence of a net charge on the two surfaces produces an energy barrier in the interaction potential curve at larger distances, as has been discussed before. The transition from a repulsive to an attractive interaction, at close plate proximity, occurs at just over 40% renneting in our model system. Experimental results put this value at 80% (Brulë, Lenoir, & Remeuf, 2000) and in some cases as high as 95%. However, it turns out that the percentage value for the renneting at the transition point is a very sensitive function of κ-casein surface coverage. For example, at a value of Γ=0.0032 chains per monomer unit area, our calculations already provide a percentage value of ~ 87% for the transition, not far from the experimental data reported by Dalgleish (1979). At much higher values of Γ no transition is obtained at all and the interactions remain repulsive even when all of the KP chains are replaced with PKC. Indeed, this was the limit at which Mellema et al. (1999) had carried out the first study of κ-casein covered surfaces using SCF method. Our calculations, performed at a degree of coverage Γ=0.01 chains/a_0^2, demonstrates this point rather clearly. The results are presented in Fig. 9. The value of Γ used is still only half as much as the one assumed by Mellema et al. (1999), but even at this level of coverage, the steric repulsion forces generated by both KC and PKC layers completely dominate over the van der Waals attraction between the hydrophobic surfaces. The van der Waals interaction is included in Fig. 9 on a separate graph, represented by the short dashed line, for comparison. At these values of Γ, both types of layers involve highly extended protein chains in the so called "brush" type conformations. Overlap of such layers is known to lead to very strong steric forces and this is clearly being manifested in the interaction curves of Fig. 9.

5. Summary and conclusions

Self consistent Field calculations, comparing the forces mediated by overlapping layers of κ-casein and para-κ-casein on two approaching hydrophobic surfaces, show that at close separations the interactions due to κ-casein (KP) are repulsive whereas those involving para-κ-casein (PKC) become attractive. The calculations were performed at neutral pH and at electrolyte concentrations typical of those in milk, with the κ-casein surface coverage estimated to be that on the surface of casein micelle. At larger separation distances, the

interaction potential curve for PKC exhibits an energy barrier, very similar to those seen from a combination of electrostatic repulsion and an attractive force, as for example in DLVO theory of colloidal stability. The electrostatic origin of this energy barrier was demonstrated by studying both systems at higher salt concentrations. With a higher background electrolyte, the energy barrier all but disappears leaving the para-κ-casein mediated interaction purely attractive. For κ-casein, the range of interaction decreases upon the addition of salt, but the interaction remains essentially repulsive. This tends to point to a strong steric component to the forces produced by κ-casein layers. It is found that the distribution of charge on κ-casein chains is quite asymmetrical. While the protein is overall negatively charged at neutral pH, para-κ-casein side of the molecule (residues 1-105) is positively charged, with most of the negative charge of the κ-casein residing on the glycomacropeptide side. Otherwise neutral surfaces, covered with KP become negatively charged. This contributes to the repulsion, but the effect is relatively small and masked by the stronger steric component. For para-κ-casein, produced during renneting, the surfaces become positively charged. However, in this case the steric repulsion is very small or non-existent, and there is more attraction due to bridging as well as the more hydrophobic nature of PKC. Here the electrostatic component is the only real contributor to the repulsive force, which manifests itself in the salt sensitive energy barrier we find in the interaction potential curves for para-κ-casein. The importance of glycopeptides nature of KP in provision of this steric interaction was demonstrated by considering forces produced by a modified κ-casein (MKC), in which we had removed the carbohydrate side chains of the protein while maintaining all the amino acid residues. The interactions were seen to become attractive without the presence of sugar moieties.

We believe that the uneven nature of the charge distribution along the κ-casein has important implications for the behaviour of this protein on interfaces. Our results, involving the calculation of the average distance of each monomer along the protein away from the surface, shows κ-casein to lie rather flat on uncharged hydrophobic surfaces. While the carbohydrate side chains and the parts of KP around these moieties do protrude away from the interface, to an extent that is enough to provide some degree of steric repulsion, the conformation of κ-casein is far from the ideal diblock configuration one predicts for β-casein, using this very same type of calculations. We have not observed a tail end of κ-casein sticking away from the surface, and the extent to which the protein protrudes away from the interface is found to be much smaller than that reported in the literature. As an emulsifier and

steric stabiliser of emulsion droplets, κ-casein is known to be less effective than β-casein, and even α_{s1}-casein. Uncharged hydrophobic surfaces used in our calculations are in some respect closer to the surface of these oil droplets. The question then is what turns κ-casein into such a good stabiliser of casein micelles when present on the surfaces of these particular particles. It is clear that this cannot be purely due to the hydrophobic or hydrophilic nature of para-κ-casein side and glycomacropeptide part of the chain. If it was, then κ-casein would be expected to be almost as good a steric stabiliser on the surface of oil droplets as is β-casein, taking up the ideal diblock type configuration on the surface of the droplets. Our calculations suggest that the asymmetrical distribution of charge, hitherto not accounted for in the conventional "hairy" κ-casein layer models (Walstra, 1990), may be just as important in determining the functional behaviour of κ-casein.

Casein micelles have additional negative charges on their surface arising from other casein fractions beside κ-casein, at neutral pH. Therefore the surface will tend to attract the positively charged side of the κ-casein (i.e. the para-κ-casein side), making it lie flat at such interfaces. In contrast the negative side, the glycomacropeptide side will be repelled and as a result will protrude into the solution far more than it will otherwise do if on an uncharged surface. This gives rise to the diblock type configuration for κ-casein one expects and results in the strong steric forces between the micelles. Without the glycomacropeptide side of course, the positively charged PKC by itself lies too flat on the surface to provide any steric repulsion. There is an implication for electrostatic forces too, though overall this is a less significant component of repulsive interactions. At pH of milk, the additional negative charge provided by other casein fractions, reinforces the net negative charge of κ-casein on the surface, thus enhancing the electrostatic component of repulsion. On the other hand, the positive charge of para-κ-casein only serves to reduce the overall surface charge, partially neutralising some of the charge arising from the other casein fractions. Thus renneting reduces both steric and electrostatic components of the repulsive force. Currently our SCF calculations, reported in this paper, are being extended to charged surfaces in order to examine the above scenario. Initial results do provide tentative support for the proposed picture. In the meantime, experimental work involving ζ-potentials measurements of partially renneted κ-casein covered oil droplets, with no inherent charge of their own, should provide the most direct test of our results so far.

Acknowledgments

Many useful discussions with E. Dickinson and A. Akinshina are gratefully acknowledged. We also thank B.S. Murray, M. Corredig and C.G. de Kruif for their helpful comments.

References

Akhtar, M., & Dickinson, E. (2007). Whey protein-maltodextrin conjugates as emulsifying agents: An alternative to gum arabic. *Food Hydrocolloids, 21*(4), 607-616.

Akinshina, A., Ettelaie, R., Dickinson, E., & Smyth, G. (2008). Interactions between Adsorbed Layers of alpha(S1)-Casein with Covalently Bound Side Chains: A Self-Consistent Field Study. *Biomacromolecules, 9*(11), 3188-3200.

Alexander, M., Rojas-Ochoa, L. F., Leser, M., & Schurtenberger, P. (2002). Structure, dynamics, and optical properties of concentrated milk suspensions: An analogy to hard-sphere liquids. *Journal of Colloid and Interface Science, 253*(1), 35-46.

Atkinson, P. J., Dickinson, E., Horne, D. S., Leermakers, F. A. M., & Richardson, R. M. (1996). Theoretical and experimental investigations of adsorbed protein structure at a fluid interface. *Berichte Der Bunsen-Gesellschaft-Physical Chemistry Chemical Physics, 100*(6), 994-998.

Bak, M., Rasmussen, L. K., Petersen, T. E., & Nielsen, N. C. (2001). Colloidal calcium phosphates in casein micelles studied by slow-speed-spinning P-31 magic angle spinning solid-state nuclear magnetic resonance. *Journal of Dairy Science, 84*(6), 1310-1319.

Brulë, G., Lenoir, J., & Remeuf, F. (2000). The casein micelle and milk coagulation. In E. Andre & G. Jean-Claude (Eds.), *Cheese making: from science to quality assurance* (second ed., pp. 7-40). Paris: Lavoisier

Cooper, C., Corredig, M., & Alexander, M. (2010). Investigation of the Colloidal Interactions at Play in Combined Acidification and Rennet of Different Heat-Treated Milks. *Journal of Agricultural and Food Chemistry, 58*(8), 4915-4922.

Dalgleish, D. G. (1979). Proteolysis and aggregation of casein micelles treated with immobilised or soluble chymosin. *Journal of Dairy Research, 46*(4), 653-661.

Dalgleish, D. G. (1984). Measurement of electrophoretic mobilities and zeta-potentials of particles from milk using laser doppler electrophoresis. *Journal of Dairy Research, 51*(3), 425-438.

Dalgleish, D. G. (2011). On the structural models of bovine casein micelles-review and possible improvements. *Soft Matter, 7*(6), 2265-2272.

Dalgleish, D. G., & Corredig, M. (2012). The Structure of the Casein Micelle of Milk and Its Changes During Processing. In M. P. Doyle & T. R. Klaenhammer (Eds.), *Annual Review of Food Science and Technology, Vol 3* (Vol. 3, pp. 449-467). Palo Alto: Annual Reviews.

Dalgleish, D. G., & Hallett, F. R. (1995). Dynamic light scattering - Applications to food systems. *Food Research International, 28*(3), 181-193.

Dalgleish, D. G., Spagnuolo, P. A., & Goff, H. D. (2004). A possible structure of the casein micelle based on high-resolution field-emission scanning electron microscopy. *International Dairy Journal, 14*(12), 1025-1031.

de Kruif, C. G., Huppertz, T., Urban, V. S., & Petukhov, A. V. (2012). Casein micelles and their internal structure. *Advances in Colloid and Interface Science, 171-172*, 36-52.

de Kruif, C. G., & Zhulina, E. B. (1996). kappa-casein as a polyelectrolyte brush on the surface of casein micelles. *Colloids and Surfaces a-Physicochemical and Engineering Aspects, 117*(1-2), 151-159.

Dewan, R. K., Chudgar, A., Mead, R., Bloomfield, V. A., & Morr, C. V. (1974). Molecular weight and size distribution of bovine milk casein micelles *Biochemica et Biophysica Acta., 342*, 313-321.

Dickinson, E., Horne, D. S., Pinfield, V. J., & Leermakers, F. A. M. (1997). Self-consistent-field modelling of casein adsorption - Comparison of results for alpha(s1)-casein and beta-casein. *Journal of the Chemical Society-Faraday Transactions, 93*(3), 425-432.

Dickinson, E., Pinfield, V. J., Horne, D. S., & Leermakers, F. A. M. (1997). Self-consistent-field modelling of adsorbed casein Interaction between two protein-coated surfaces. *Journal of the Chemical Society-Faraday Transactions, 93*(9), 1785-1790.

Dickinson, E., & Semenova, M. G. (1992). Emulsifying properties of covalent protein dextran hybrids. *Colloids and Surfaces, 64*(3-4), 299-310.

Donnelly, W. J., McNeill, G. P., Buchheim, W., & McGann, T. C. A. (1984). A comprehensive study of the relationship between size and protein-composition in natural bovine casein micelles. *Biochimica Et Biophysica Acta, 789*(2), 136-143.

Ettelaie, R., Akinshina, A., & Dickinson, E. (2008). Mixed protein-polysaccharide interfacial layers: a self consistent field calculation study. *Faraday Discussions, 139*, 161-178.

Ettelaie, R., Akinshina, A., & Dickinson, E. (2009). A theoretical self-consistent field study of mixed interfacial biopolymer films. In Q. Huang, P. Given & M. Qian (Eds.), *Micro/Nanoencapsulation of active food ingredients* (Vol. 1007, pp. 46-66): American Chemical Society.

Ettelaie, R., Akinshina, A., & Maurer, S. (2012). Mixed protein−polysaccharide interfacial layers: effect of polysaccaride charge distribution. *Soft Matter, 8*(29), 7582–7597.

Ettelaie, R., Murray, B. S., & James, E. L. (2003). Steric interactions mediated by multiblock polymers and biopolymers: role of block size and addition of hydrophilic side chains. *Colloids and Surfaces B-Biointerfaces, 31*(1-4), 195-206.

Evers, O. A., Scheutjens, J., & Fleer, G. J. (1990). Statistical thermodynamics of block copolymer adsorption .1. formulation of the model and results for adsorbed layer sructure. *Macromolecules, 23*(25), 5221-5233.

Farrell, H. M., Malin, E. L., Brown, E. M., & Qi, P. X. (2006). Casein micelle structure: What can be learned from milk synthesis and structural biology? *Current Opinion in Colloid & Interface Science, 11*(2-3), 135-147.

Fleer, G. J., Cohen Stuart, M. A., Scheutjens, J. M. H. M., Cosgrove, T., & Vincent, B. (1993). *Polymers at interfaces*. London: Chapman and Hall.

Fox, P. F., McSweeney, P., Cogan, T., & Guinee, T. (2004). Cheese: Chemistry, Physics and Microbiology : Volume 1, General Aspects (Third ed.): Academic Press

Grossberg, A. Y., & Khokhlov, A. R. (1994). *Statistical physics of macromolecules*. New York: AIP press.

Gulseren, I., Alexander, M., & Corredig, M. (2010). Probing the colloidal properties of skim milk using acoustic and electroacoustic spectroscopy. Effect of concentration, heating and acidification. *Journal of Colloid and Interface Science, 351*(2), 493-500.

Horne, D. S. (2006). Casein micelle structure: Models and muddles. *Current Opinion in Colloid & Interface Science, 11*(2-3), 148-153.

Hunter, R. J. (1989). *Foundations of Colloid Science* (Vol. 1). Oxford: Clarendon.

Jolles, P., & Fiat, A. M. (1979). The carbohydrate portions of Milk glycoproteins. *Journal of Dairy Research, 46*, 187-191.

Kalab, M. (1993). Practical aspects of electron-microscopy in dairy research. *Food Structure, 12*(1), 95-114.

Leermakers, F. A. M., Atkinson, P. J., Dickinson, E., & Horne, D. S. (1996). Self-consistent-field modeling of adsorbed beta-casein: Effects of pH and ionic strength on surface coverage and density profile. *Journal of Colloid and Interface Science, 178*(2), 681-693.

Lucey, J. A., Gorry, C., Okennedy, B., Kalab, M., TanKinita, R., & Fox, P. F. (1996). Effect of acidification and neutralization of milk on some physico-chemical properties of casein micelles. *International Dairy Journal, 6*(3), 257-272.

Mellema, M., Leermakers, F. A. M., & de Kruif, C. G. (1999). Molecular mechanism of the renneting process of casein micelles in skim milk, examined by viscosity and light-scattering experiments and simulated by model SCF calculations. *Langmuir, 15*(19), 6304-6313.

Mercier, J. C., Brignon, G., & Ribadeau.B. (1973). Primary structure of bovine kappa-casein - complete sequence. *European Journal of Biochemistry, 35*(2), 222-235.

Ouanezar, M., Guyomarc'h, F., & Bouchoux, A. (2012). AFM Imaging of Milk Casein Micelles: Evidence for Structural Rearrangement upon Acidification. *Langmuir, 28*(11), 4915-4919.

Parkinson, E. L., Ettelaie, R., & Dickinson, E. (2005). Using self-consistent-field theory to understand enhanced steric stabilization by casein-like copolymers at low surface coverage in mixed protein layers. *Biomacromolecules, 6*(6), 3018-3029.

Patel, P. A., Jeon, J., Mather, P. T., & Dobrynin, A. V. (2006). Molecular dynamics simulations of multilayer polyelectrolyte films: Effect of electrostatic and short-range interactions. *Langmuir, 22*(24), 9994-10002.

Scheutjens, J., & Fleer, G. J. (1980). Statistical-theory of the adsorption of interacting chain molecules .2. train, loop, and tail size distribution. *Journal of Physical Chemistry, 84*(2), 178-190.

Scheutjens, J., & Fleer, G. J. (1982). Effect of polymer adsorption and depletion on the interaction between 2 parallel surfaces. *Advances in Colloid and Interface Science, 16*(JUL), 361-380.

Swaisgood, H. E. (2003). Chemistry of the caseins. In P. F. Fox & P. L. H. McSweeney (Eds.), *Advanced Diary chemistry : proteins* (Vol. 1). New York: Kluwer academic.

Tuinier, R., & de Kruif, C. G. (2002). Stability of casein micelles in milk. *Journal of Chemical Physics, 117*(3), 1290-1295.

Wade, T., Beattie, J. K., Rowlands, W. N., & Augustin, M. A. (1996). Electroacoustic determination of size and zeta potential of casein micelles in skim milk. *Journal of Dairy Research, 63*(3), 387-404.

Walstra, P. (1979). The voluminosity of bovine casein micelles and some of its implications. *Journal of Dairy Research, 46*, 317-323.

Walstra, P. (1990). On the stability of casein micelles. *Journal of Dairy Science, 73*(8), 1965-1979.

Zhulina, E. B., & Leermakers, F. A. M. (2007). A self-consistent field analysis of the neurofilament brush with amino-acid resolution. *Biophysical Journal, 93*(5), 1421-1430.

Zhulina, E. B., & Leermakers, F. A. M. (2009). On the polyelectrolyte brush model of neurofilaments. *Soft Matter, 5*(15), 2836-2840.

Figure captions

Fig. 1. Schematic diagram of the primary sequence of κ-casein, displaying its amino acid residues classified according to the five distinct groups used in our model. The arrow shows the position of the residue 142, to which the carbohydrate side chains of our model κ-casein are attached.

Fig. 2. Interaction potential between two flat surfaces, arising from the overlap of κ-casein layers (solid line), para-κ-casein layers (long dashed line) and κ-casein without its carbohydrate side chains (dashed-dotted line). The surface coverage was Γ=0.0025 chains per monomer area, pH=7 and the electrolyte volume fraction 0.0015. The graph for the van der Waals interaction has also been included for comparison (short dashed line).

Fig. 3. As in Fig. 2, but at a higher salt volume fraction of 0.0045 and without the graph for the modified κ-casein.

Fig. 4. Variation of the electrical potential (in units of k_BT/e) as a function of distance away from the interface for κ-casein (solid line) and para-κ-casein (long dashed line) systems of Fig. 2.

Fig. 5. Variation of charge (in units of e) of κ-casein (solid line) and para-κ-casein (long dashed line) with pH of the solution.

Fig. 6. Graphs showing the drop in the volume fraction of the protein in the interfacial region, with distance away from the surface for κ-casein layers (solid line), para-κ-casein layers

(long dashed line) and κ-casein without its carbohydrate side chains (dashed-dotted line). The results are calculated at the same conditions as the systems in Fig. 2.

Fig. 7. The average distance away from the surface for each of the amino acid residue of the κ-casein, residing on a hydrophobic interface. The residues are numbered 1 to 169, starting from the N-terminus end of the protein. Fig. 7a shows the results for the full κ-casein with its sugar moieties included. The positions of these moieties are indicated by the dashed line. Fig. 7b displays the same data but for modified κ-casein without its carbohydrate side chains. Both results were obtained at neutral pH and a salt volume fraction of 0.0015. The graphs are to be compared with those obtained by Dickinson et al. (1997) for α_{s1}-casein and β-casein, using a similar method.

Fig. 8. The change in the interaction potential between two flat surfaces at different stages of renneting. The label on each graph indicates the percentage of κ-casein chains that have been converted to para-κ-casein ones. The results were calculated under the same pH and electrolyte conditions as those in Fig. 2.

Fig. 9. The same graphs as those in Fig. 2, but now at a higher surface coverage of Γ=0.01 chains per monomer area. The graphs show that at this level of surface coverage, the interaction potentials for both κ-casein and para-κ-casein are strongly repulsive.

Table 1. List of Flory-Huggins χ parameters used in our model specifying the strength of the short range nearest neighbour interactions between different monomer groups. Also shown are the pK_a values for each ionisable group.

Figure 1

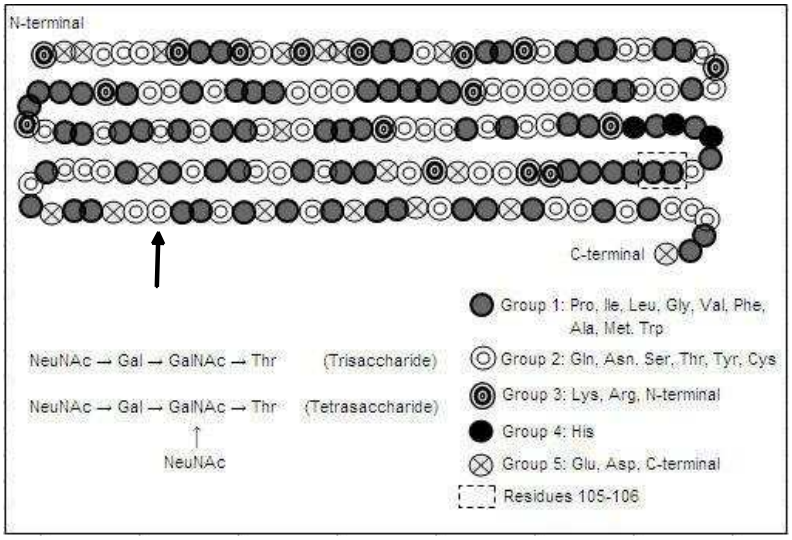
N-terminal
C-terminal
NeuNAc → Gal → GalNAc → Thr (Trisaccharide)
NeuNAc → Gal → GalNAc → Thr (Tetrasaccharide)
NeuNAc
Group 1: Pro, Ile, Leu, Gly, Val, Phe, Ala, Met, Trp
Group 2: Gln, Asn, Ser, Thr, Tyr, Cys
Group 3: Lys, Arg, N-terminal
Group 4: His
Group 5: Glu, Asp, C-terminal
Residues 105-106

Figure 2

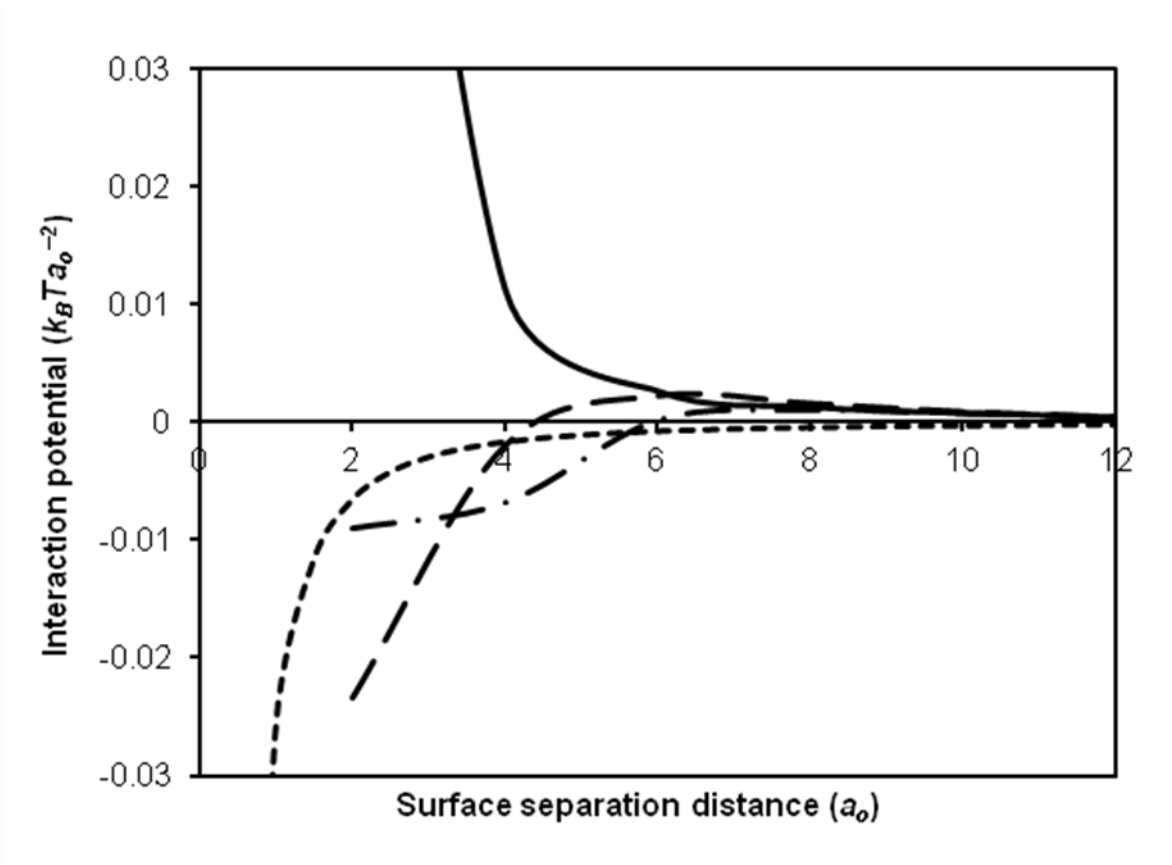
0.03
0.02
0.01
0
-0.01
-0.02
-0.03
0
2
4
6
8
10
12
Interaction potential ($k_BTa_o^{-2}$)
Surface separation distance (a_o)

Figure 3

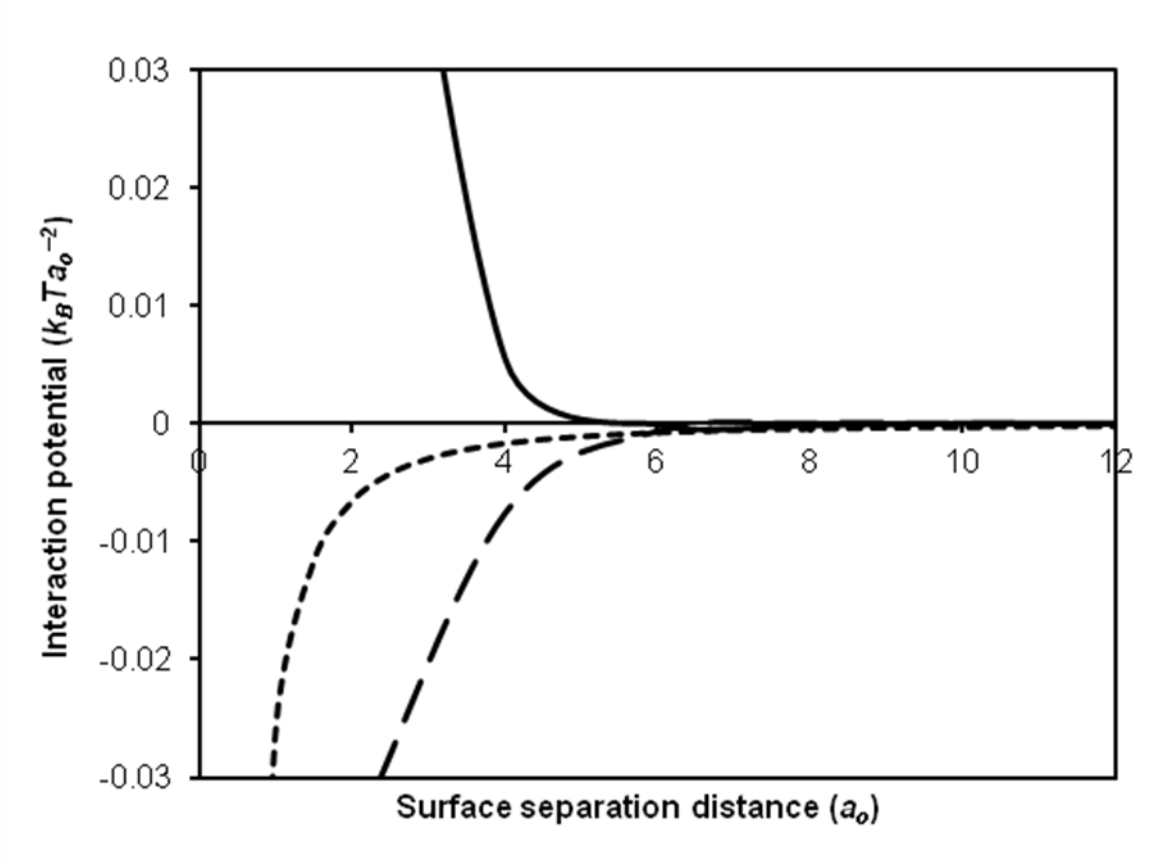
0.03
0.02
0.01
0
-0.01
-0.02
-0.03
0
2
4
6
8
10
12
Interaction potential ($k_BTa_o^{-2}$)
Surface separation distance (a_o)

Figure 4

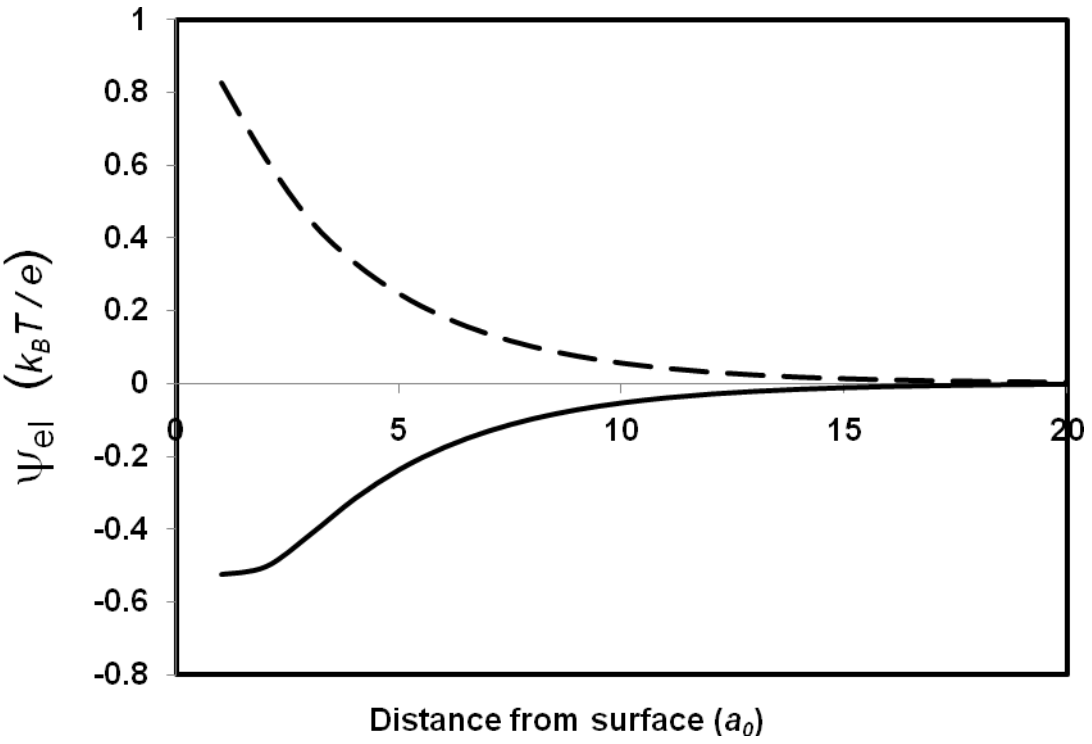
1
0.8
0.6
0.4
0.2
0
-0.2
-0.4
-0.6
-0.8
0
5
10
15
20
ψ_{el} $(k_B T/e)$
Distance from surface (a_0)

Figure 5

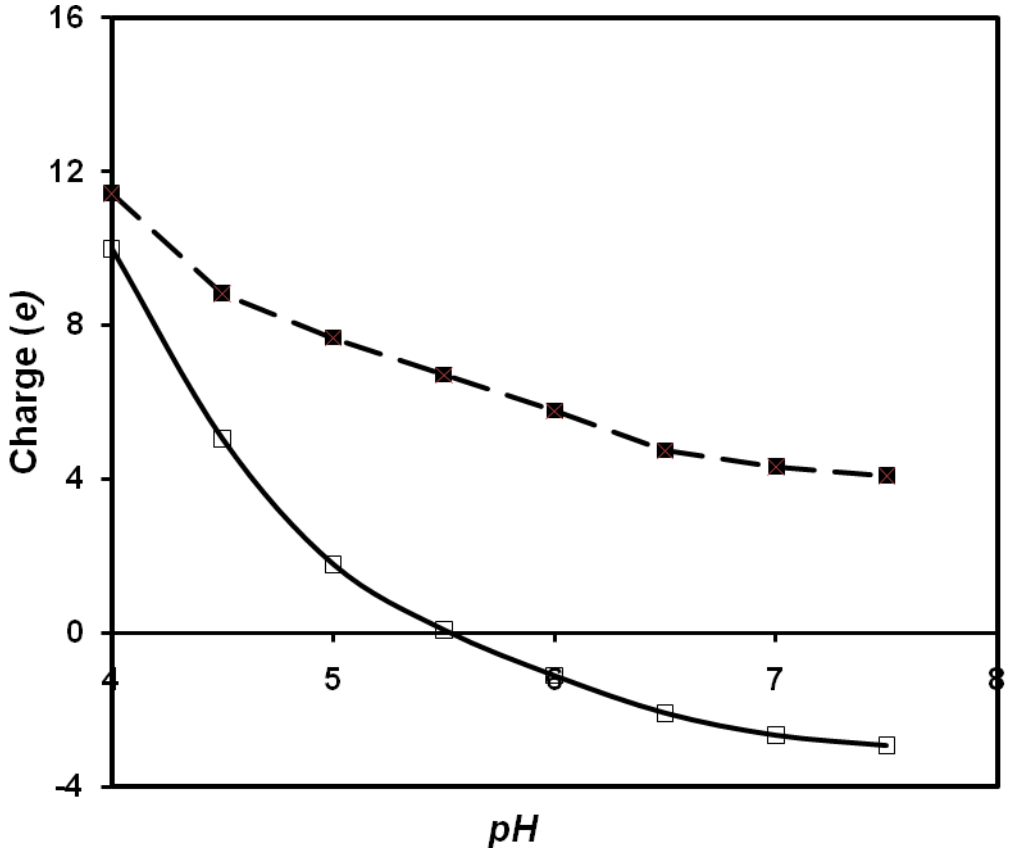

Figure 6

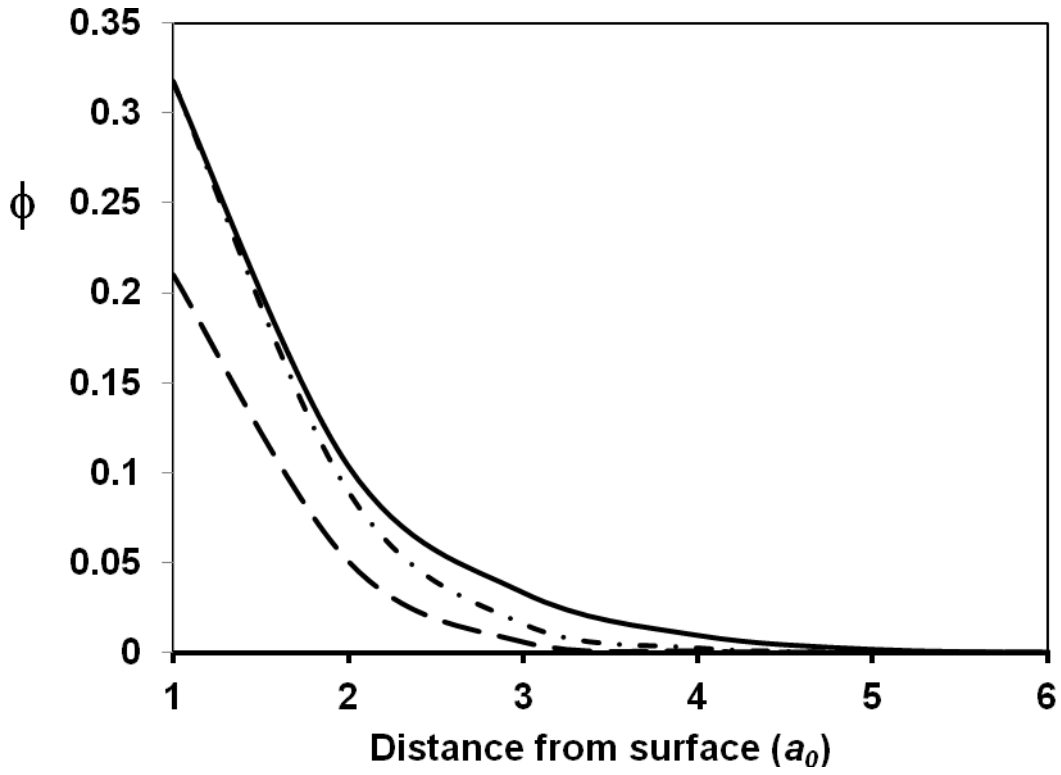

Figure 7a

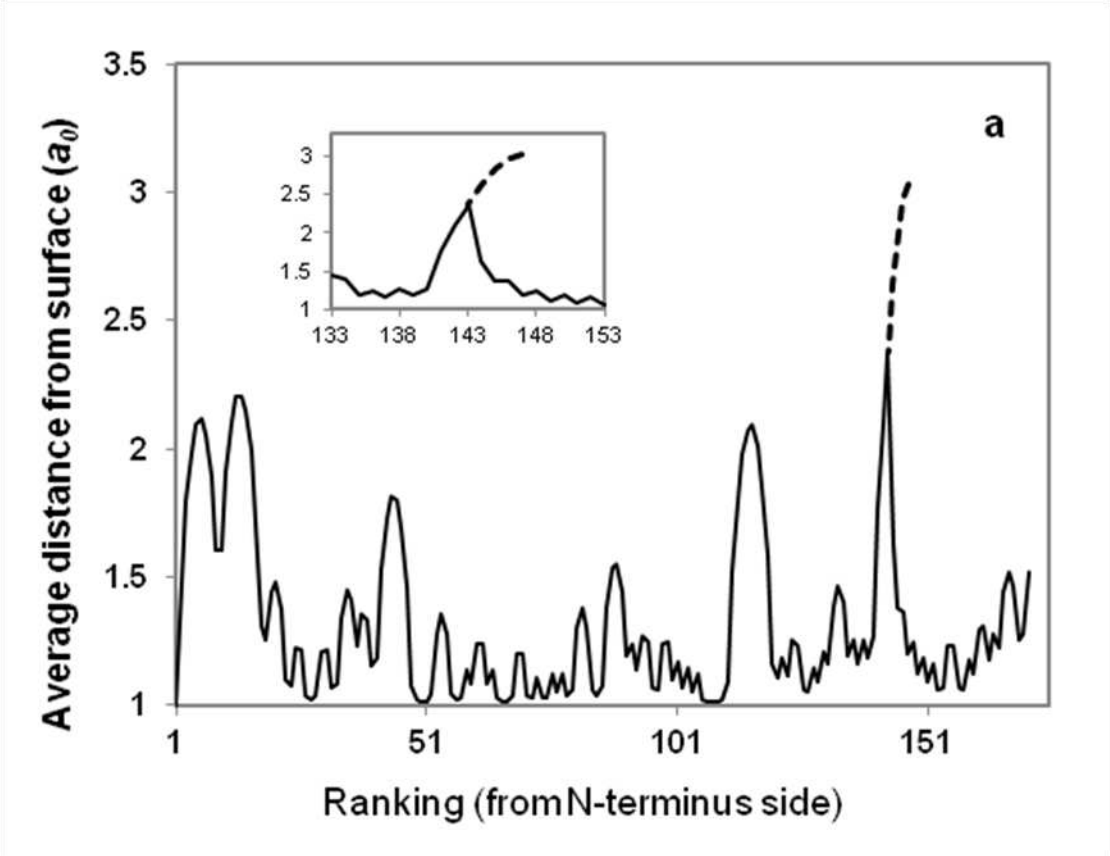
a
Average distance from surface (a_0)
3.5
3
2.5
2
1.5
1
1
51
101
151
Ranking (from N-terminus side)
3
2.5
2
1.5
1
133
138
143
148
153

Figure 7b

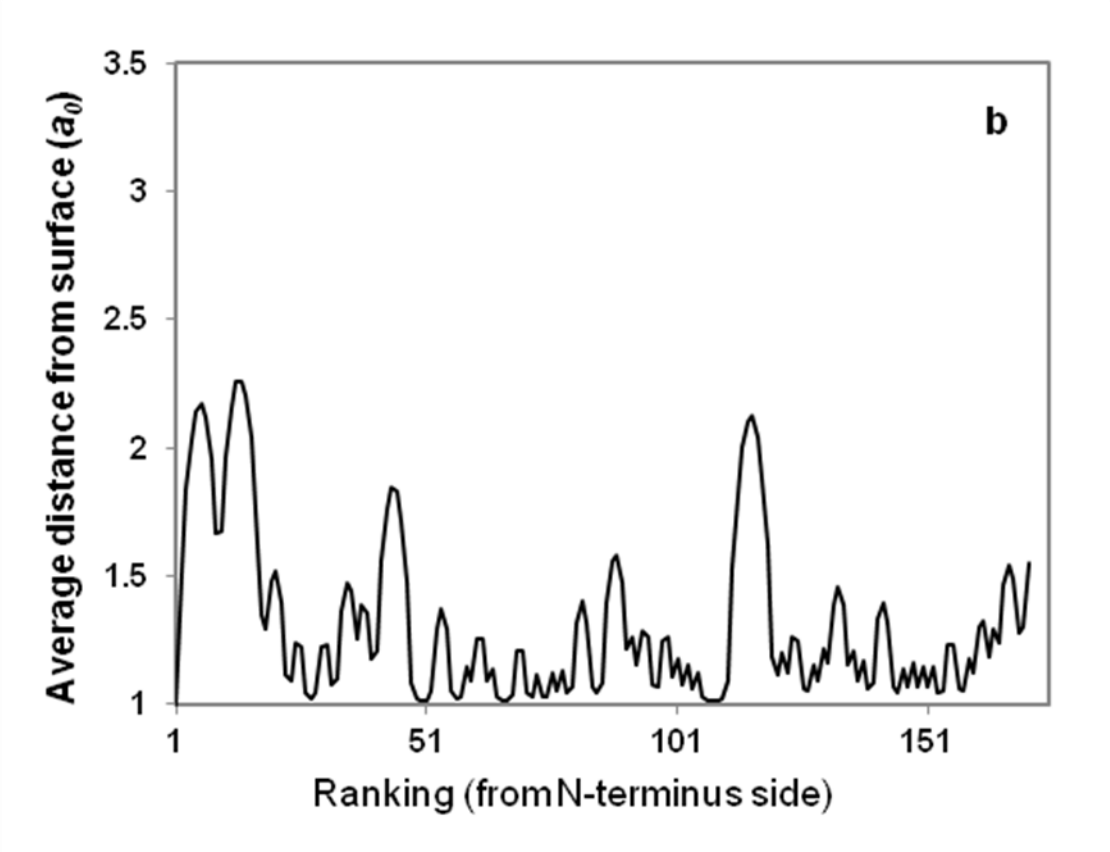
b
Average distance from surface (a_0)
3.5
3
2.5
2
1.5
1
1
51
101
151
Ranking (from N-terminus side)

Figure 8

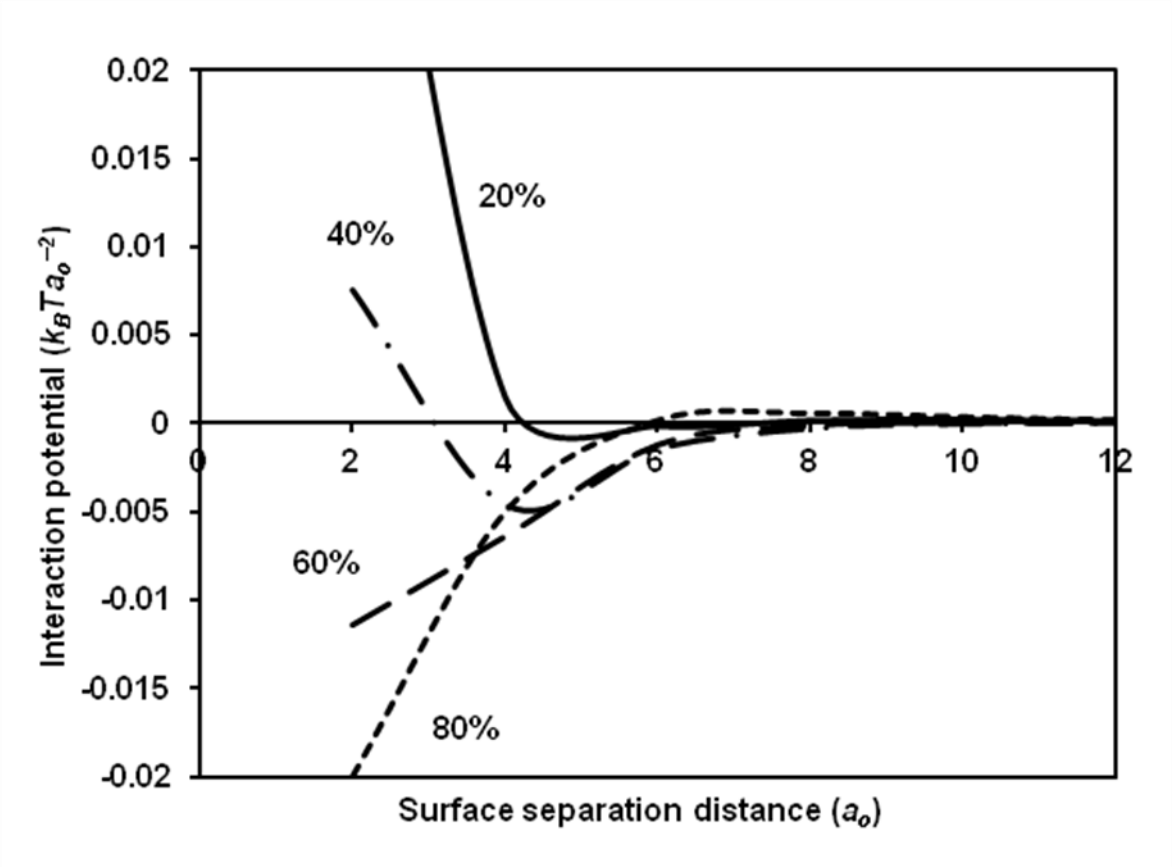
0.02
0.015
0.01
0.005
0
-0.005
-0.01
-0.015
-0.02
0
2
4
6
8
10
12
20%
40%
60%
80%
Interaction potential ($k_B T a_o^{-2}$)
Surface separation distance (a_o)

Figure 9

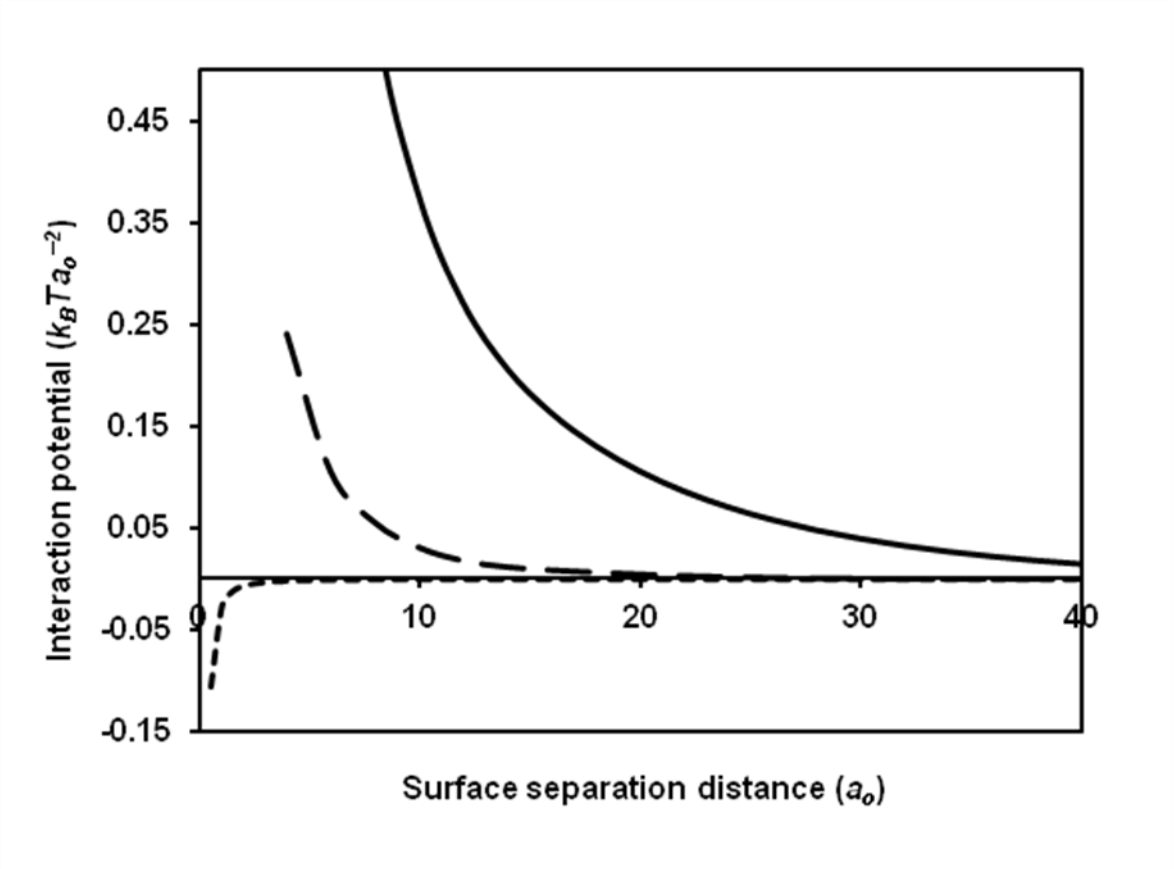
0.45
0.35
0.25
0.15
0.05
-0.05
-0.15
0
10
20
30
40
Interaction potential ($k_BTa_o^{-2}$)
Surface separation distance (a_o)

Table 1

Monomer type	**0**	**1**	**2**	**3**	**4**	**5**	**6**	**7**	**8**
0- Solvent	0	1.0	0	0	0	0	0	-1	-1
1- Hydrophobic residues	1.0	0	2.0	2.5	2.5	2.5	2.5	2.5	2.5
2- Polar residues	0	2.0	0	0	0	0	0	0	0
3- Positive residues	0	2.5	0	0	0	0	0	0	0
4- Histidine	0	2.5	0	0	0	0	0	0	0
5- Negative residues	0	2.5	0	0	0	0	0	0	0
6- Carbohydrate Groups	0	2.5	0	0	0	0	0	0	0
7- Ion (+)	-1.0	2.5	0	0	0	0	0	0	0
8- Ion (-)	-1.0	2.5	0	0	0	0	0	0	0
Surface	0	-2	0	0	0	0	0	0	0
pKa	-	-	-	10	6.1	4.1	-	-	-